

UC San Diego

UC San Diego Previously Published Works

Title

Atlas of plasma metabolic markers linked to human brain morphology

Permalink

<https://escholarship.org/uc/item/1cj706ph>

Authors

van der Meer, Dennis

Kopal, Jakub

Shadrin, Alexey A

et al.

Publication Date

2025-01-14

DOI

10.1101/2025.01.12.632645

Atlas of plasma metabolic markers linked to human brain morphology

Dennis van der Meer, Ph.D.^{1*}, Jakub Kopal, Ph.D.¹, Alexey A. Shadrin, Ph.D.^{1,2}, Julian Fuhrer, Ph.D.¹, Jaroslav Rokicki, Ph.D.³, Sara E. Stinson, Ph.D.¹, Srdjan Djurovic, Ph.D.^{1,2,4}, Anders M. Dale, Ph.D.⁵ & Ole A. Andreassen, M.D. Ph.D.^{1,2*}

¹Centre for Precision Psychiatry, Division of Mental Health and Addiction, Oslo University Hospital & Institute of Clinical Medicine, University of Oslo, Oslo, Norway

²K.G. Jebsen Centre for Neurodevelopmental Disorders, University of Oslo and Oslo University Hospital, Oslo, Norway

³Centre of Research and Education in Forensic Psychiatry (SIFER), Oslo University Hospital, Oslo, Norway

⁴Department of Medical Genetics, Oslo University Hospital, Oslo, Norway

⁵Center for Multimodal Imaging and Genetics, University of California at San Diego, La Jolla, CA 92037, USA

*Corresponding author: [dennisva\[at\]uio.no](mailto:dennisva[at]uio.no) & [ole.andreassen\[at\]medisin.uio.no](mailto:ole.andreassen[at]medisin.uio.no). Address: Kirkeveien 166, 0450 Oslo, Norway

ABSTRACT

Background: Metabolic processes form the basis of the development, functioning and maintenance of the brain. Despite accumulating evidence of the vital role of metabolism in brain health, no study to date has comprehensively investigated the link between circulating markers of metabolic activity and *in vivo* brain morphology in the general population.

Methods: We performed uni- and multivariate regression on metabolomics and MRI data from 24,940 UK Biobank participants, to estimate the individual and combined associations of 249 circulating metabolic markers with 91 measures of global and regional cortical thickness, surface area and subcortical volume. We investigated similarity of the identified spatial patterns with brain maps of neurotransmitters, and used Mendelian randomization to uncover causal relationships between metabolites and the brain.

Results: Intracranial volume and total surface area were highly significantly associated with circulating lipoproteins and glycoprotein acetyls, with correlations up to .15. There were strong regional associations of individual markers with mixed effect directions, with distinct patterns involving frontal and temporal cortical thickness, brainstem and ventricular volume. Mendelian randomization provided evidence of bidirectional causal effects, with the majority of markers affecting frontal and temporal regions.

Discussion: The results indicate strong bidirectional causal relationships between circulating metabolic markers and distinct patterns of global and regional brain morphology. The generated atlas of associations provides a better understanding of the role of metabolic pathways in structural brain development and maintenance, in both health and disease.

Keywords: metabolomics; brain morphology. Word count: 3120.

Metabolic processes form the basis of the development, functioning and maintenance of the brain.¹ Accordingly, there is increasing evidence that metabolic dysregulation plays a central role in the etiology of neurodevelopmental and neurodegenerative disorders. Broadly, these disorders are associated with abnormal metabolic activity and heightened levels of cardiometabolic disease.^{2,3} Markers of metabolic activity, such as lipoproteins, cholesterol, fatty acids, and glucose, are now well-captured in plasma by high-throughput nuclear magnetic resonance (NMR) spectroscopy,⁴ explaining more variance in metabolic dysfunction than traditional measurements.⁵ As the world's population is becoming progressively older and the prevalence of obesity is rising,⁶ a better understanding of the connection between metabolic markers and the brain will help to develop more specific interventions to combat these global public health challenges.

Metabolism is tightly intertwined with neuronal processes. The brain uses 25% of the body's energy derived from glucose, primarily to maintain proper ion gradients and neurotransmitter levels at the synapses.⁷ Further, amino acids act as precursors for neurotransmitters, to maintain essential synaptic functioning and plasticity.⁸ Lipids constitute 50% of the brain dry weight;⁹ they are essential components of the structure and function of the brain,¹⁰ as they facilitate signal conductance and synaptic throughput.^{11,12} The brain is involved in controlling metabolic activity, by both cortical and subcortical circuitry, controlling food intake and energy expenditure.¹³ This is evidenced by extensive molecular crosstalk between the brain and somatic metabolic systems.¹⁴

We and others have mapped widespread associations of measures of cardiometabolic risk factors, such as body mass index (BMI), with macro-scale brain structure.¹⁵ In line with these results, several small-

scale studies have found that plasma levels of specific markers are associated with regional brain structure, especially prefrontal volume. This includes high- and low-density lipoproteins (HDL, LDL),^{16–18} glutamate and glutamine,¹⁹ and inflammatory markers.²⁰ Studies of post-mortem brain tissue of individuals with psychiatric disorders have also reported abnormal metabolic marker levels in the prefrontal cortex, striatum and thalamus.^{21–23} These results have been complemented by two-sample Mendelian randomization studies, finding evidence of causal effects of circulating lipids on cortical morphology.^{24,25}

Despite accumulating evidence of the important connection between metabolic processes and brain health, no study to date has comprehensively investigated the link between circulating metabolic markers and *in vivo* brain morphology in the general population. Here, we examine the associations of 249 NMR-derived measures of plasma metabolite concentrations with MRI-derived measures of cortical thickness, surface area and subcortical volume, using data from nearly twenty five thousand UK Biobank (UKB) participants. In addition to uncovering strong, widespread associations between a range of metabolic markers and brain morphology, we identify specific spatial patterns with functional implications and provide evidence of bidirectional causal relationships. This work offers novel insights into the metabolic underpinnings of brain development and maintenance, identifying potential targets for therapeutic intervention common to metabolic and brain disorders.

Results

Our study sample consisted of 24,940 UK Biobank participants (mean age at scan 64.0 years, 52.5% female) that had both T1 brain MRI and NMR metabolomics data. The T1 data was processed through

Freesurfer, from which we extracted the cortical thickness and surface area of 34 cortical regions, following the Desikan-Killiany parcellation,²⁶ as well as the volume of 20 subcortical regions, and 3 global brain measures.²⁷ The NMR data consisted of the Nightingale panel of metabolic markers,⁴ encompassing 228 lipids, lipoproteins or fatty acids and 21 non-lipid traits, namely amino acids, ketone bodies, fluid balance, glycolysis-, and inflammation-related metabolic markers,²⁸ see Supplementary Table 1 and 2 for an overview of all included brain measures and metabolic markers, with abbreviations and categorizations. Where applicable, we adjusted p-values with the Benjamini-Hochberg method to correct for comparisons across the 249 markers and 91 brain measures, and set significance thresholds at $\alpha=.05$. All analyses were corrected for age, sex, scanner, and scan quality. Regional brain measures were additionally corrected for a metric-specific global measure (i.e., mean thickness, total surface area, or intracranial volume (ICV)).

Associations between brain morphology and metabolic markers

We first used partial least squares (PLS) regression to aggregate across all markers, identifying their joint correlation with each brain measure. The strongest correlations were seen with ICV and total surface area, followed by regional volume of ventricles and the brainstem, see **Figure 1a**. This aligned with our findings obtained using linear regression. Specifically, the majority of the 249 markers had a highly significant association with ICV ($n=192$) and total surface area ($n=183$) and, to a lesser extent, mean cortical thickness ($n=139$). Regionally, the most significant effects were on thickness of the temporal lobe and, subcortically, on the brainstem, ventricles and ventral diencephalon, see **Figure 1b**.

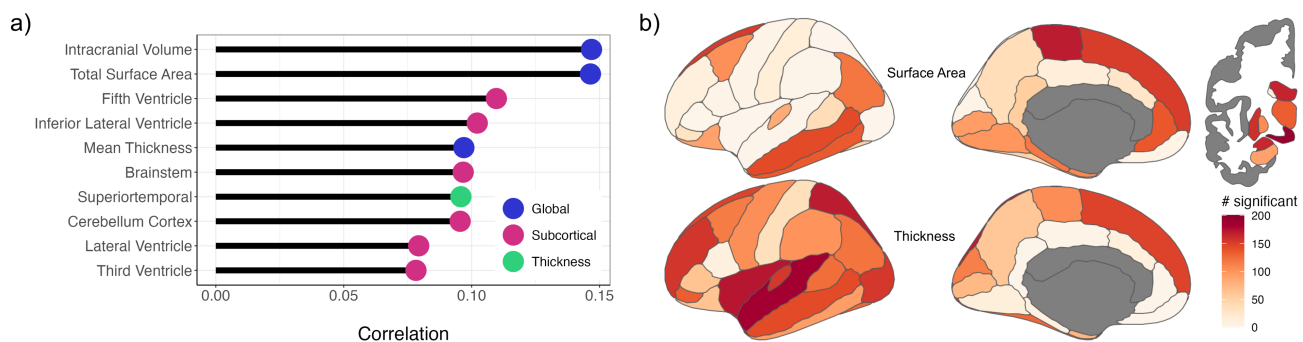


Figure 1. Association with global and regional brain morphology across all metabolic markers. a) Results of partial least squares regression, depicting the top 10 highest correlations (*x*-axis) found between all markers as a set and specific brain measures (*y*-axis). Color coding indicates the brain metric, with global in blue), subcortical in red and thickness in green. **b)** brain maps depicting the number of significant associations (color-coded) between the markers and the different regional brain measures.

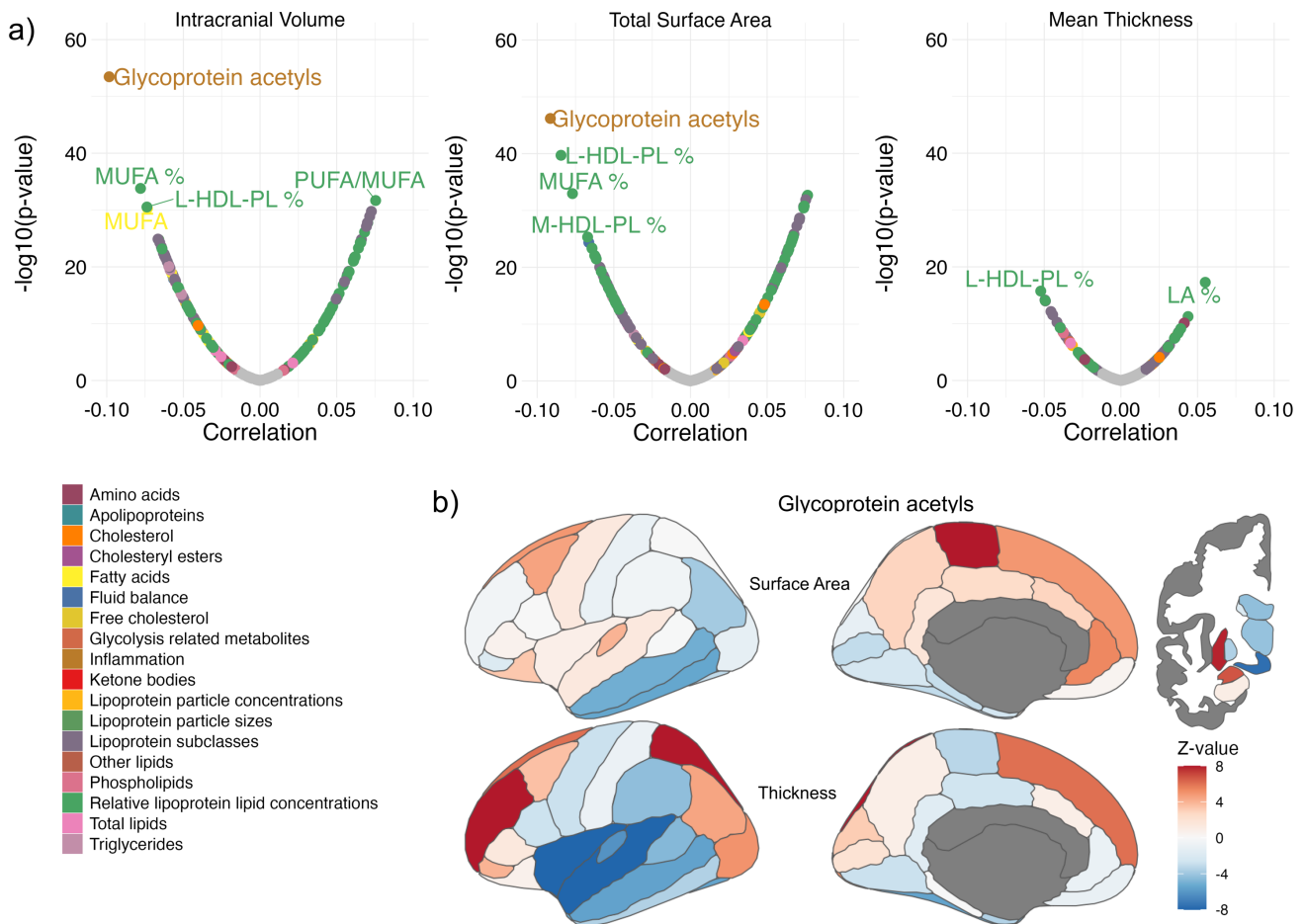


Figure 2. Associations of individual metabolic markers with global and regional brain morphology. **a)** Summary of the strength of associations between global brain measures with each individual metabolic markers (dots), expressed as correlation on the x-axis and $-\log_{10}(p\text{-value})$ on the y-axis. The color of the dots indicate the marker category, as specified in the legend, and the strongest associations are annotated with the marker name. **b)** Brain maps depicting the strength of association (z-values, color-coded) between one example marker (glycoprotein acetyls) and the different regional brain measures, to showcase individual spatial patterns.

Figure 2a highlights the strongest associations of individual markers with ICV, total surface area and mean cortical thickness. The corresponding regression coefficients were highly correlated between ICV and surface area ($r=.94$), while the correlations between mean thickness and ICV and surface area were markedly lower ($r=.19$ and $.30$ resp.). Glycoprotein acetyls stood out as the individual marker with the strongest association, explaining 1% variance in both ICV and surface area. Many markers showed strong, spatially varying associations with mixed effect directions, as evident from the example of glycoprotein acetyls shown in **Figure 2b**. We provide brain maps for each of the 249 markers that capture the spatial distributions of the identified associations across all cortical and subcortical regions in Supplementary Figure 1. Full inferential statistics are provided in Supplementary Table 3.

Given the strong correlation between subsets of markers, we ran least absolute shrinkage and selection operator (LASSO) regression on each brain measure to identify individual markers that drive the associations. This revealed that the amino acids have particularly widespread independent contributions, with glutamine influencing 32 brain measures. Global and subcortical brain measures were found to have the highest number of independent metabolites influencing them (up to 42), while regional surface area measures were all near the bottom of this ranking. The full list of markers with non-zero influences, per brain measure, is provided in Supplementary Table 4.

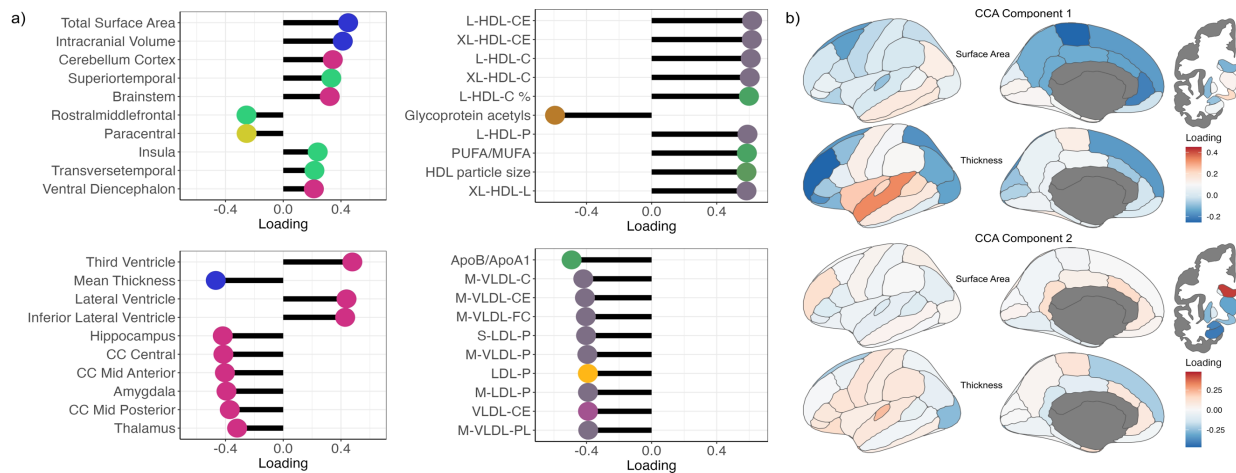


Figure 3. Shared underlying structure across all metabolic markers and brain measures. This reflects the results of the canonical correlation analysis, with an overview of loadings for component 1 and 2. **a)** on the y-axis are the ten brain measures (left panels) and metabolic markers (right panels) with the highest absolute loadings (x-axis). The colors of the dots distinguish between the brain metrics (blue for global, pink for subcortical, green for thickness, and yellow for surface area), and for marker category (grey for lipoprotein subclasses, green for relative lipoprotein concentrations, mustard for inflammation, yellow for particle concentrations, and purple for cholesteryl esters). **b)** brain maps show the spatial distributions of the loadings across cortical thickness, surface area, and subcortical volume, with loading color-coded as indicated in the legend. For both **a)** and **b)** the top row visualizes the results for component 1, and the bottom row shows component 2.

Molecular and functional pathways

We used the ‘neuromaps’ toolbox to estimate the similarity of our identified cortical spatial patterns to previously generated cortical maps of neurotransmission and brain metabolic activity. The analysis of the glycoprotein acetyls cortical thickness map, as an example of an individual marker, showed greatest similarity to maps generated through positron emission tomography (PET) studies of tracer binding to monoaminergic neurotransmission, most prominently the serotonin transporter ($r=-.54$, $p=2.3 \times 10^{-6}$) and the 5-HT1a receptor ($r=-.45$, $p=1.1 \times 10^{-4}$), as well as glucose metabolism ($r=.48$, $p=2.9 \times 10^{-5}$), see **Figure 4**.

We further analyzed the cortical maps of CCA loadings for both cortical thickness and surface area, and found that the same maps of monoaminergic neurotransmitters were among the most significantly correlated with the thickness maps of component 1 and 2. Component 1 thereby generally showed opposing directions to that of glycoprotein acetyls and component 2. For the surface area maps, we additionally found similarity with opioid receptors as well as glutamate and cannabinoid receptors. See Supplementary Table 6 for the full results.

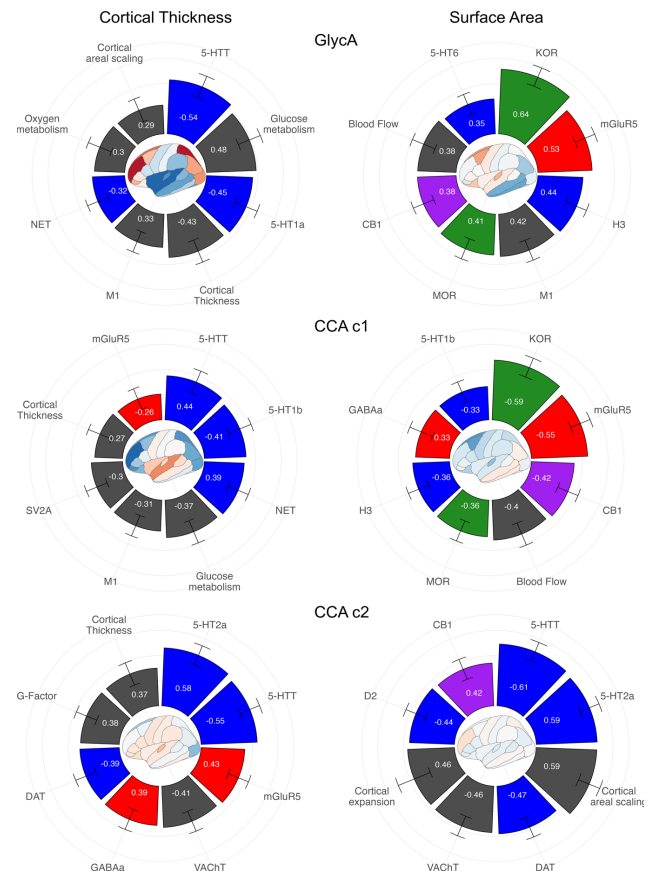


Figure 4. Coupling of the markers' regional cortical patterns to molecular and structural features of the cortex. These circular barplots show the eight highest absolute correlations between the regional cortical patterns identified in this study to previously published cortical maps, using the neuromaps repository. The top row is for the regression coefficients of glycoprotein acetyls, the middle for the loadings of the canonical correlation analysis component 1, and the bottom row for component 2. The left column shows the comparisons for the generated cortical thickness maps, and the right column for the surface area maps. The bar color coding reflects categories of neuromaps, with blue for monoaminergic neurotransmission, green for endorphins, red for amino acids, purple for endocannabinoids, and black for other.

Causal relationships

We ran a series of bidirectional Mendelian randomization (MR) analyses to determine the causal directions of the identified relationships. This generally confirmed the expected direction whereby many of the markers have a causal effect on brain morphology, most prominently on frontal and temporal cortical thickness (**Figure 5a** and **5b**). However, there were also significant influences in the opposite direction, i.e.

brain morphology measures had a causal effect on metabolic marker concentrations (**Figure 5c** and **5d**). Especially medial frontal regions together with volume of the ventral diencephalon, amygdala, and hippocampus had causal effects on markers, suggesting top down control of metabolic activity by the brain through either behavior or regulation of physiological processes.

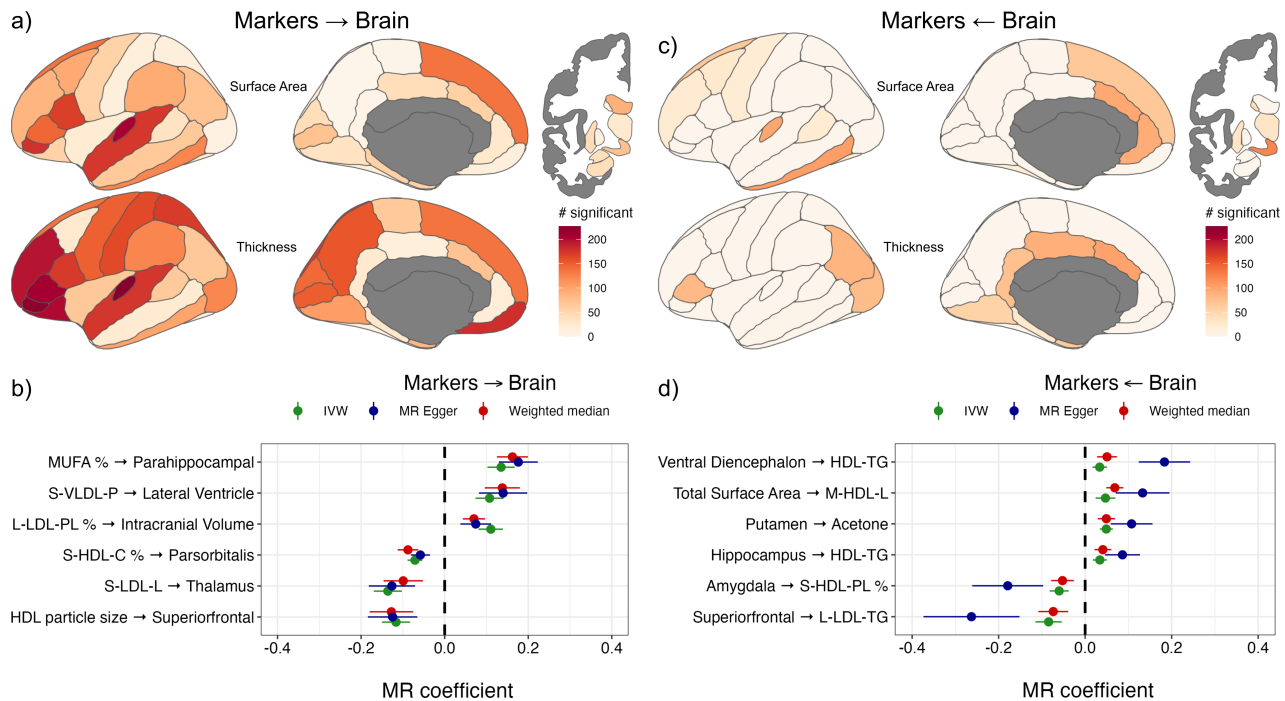


Figure 5. Causal relationships between the metabolic markers and regional brain morphology. Using Mendelian randomization, we found significant causal effects of the markers on brain morphology (**a, b**) and of brain morphology on the markers (**c, d**). The color coding of the brain maps at the top row indicates the number of significant causal relationships out of the 249 included metabolites, as indicated in the legend. The forest plots at the bottom row show the coefficients of the MR analyses on the x-axis and illustrative brain-metabolite pairs on the y-axis. The MR approach used is indicated by the coloring, as indicated in the legend.

Discussion

Here, we performed the first large-scale study of the relationship between circulating metabolic markers and *in vivo* brain morphology. We found strong evidence of widespread causal influences with spatial patterns that implicate these markers in neurodevelopmental and neurodegenerative processes. The current findings underscore the important relationship between metabolic processes and brain morphology, and indicate that markers measured in plasma can be leveraged to better understand and detect brain health.

The strongest associations, for both individual markers and as a set, were found with ICV and total cortical surface area, suggesting metabolic processes

influence global brain scaling. ICV and surface area are determined primarily early in life, followed by a decline throughout adulthood,²⁹ with an etiology that is distinct from cortical thickness.^{30,31} Specific metabolic pathways are implicated in neurodevelopmental conditions that accompany micro- or macrocephaly.³² These pathways have played a crucial role in the evolutionary expansion of the neocortex through their influence on neural progenitor cells,³³ which may partly explain the distinction between the identified associations for surface area and thickness.³⁴

Regionally, we found widespread associations, primarily with cortical thickness, with mixed effect directions, highlighting the complex nature of the relationship between the markers and brain morphology. The most prominently implicated

regions were the superior temporal and frontal lobe. These regions are among the most metabolically active and have the greatest decrease in glucose metabolism with ageing,³⁵ as well as being the most affected by age-related atrophy.³⁶ Thickness has thereby been shown to be a more sensitive metric of regional neurodegeneration than surface area.³⁷ Our findings therefore suggest that metabolomics data measured in plasma corresponds to regional differences that reflect changes in metabolic activity with age, and as such may facilitate the identification of mechanisms underlying neurodegeneration.

We found two distinct, complementary components that together explained over half of the correlation structure between the metabolites and brain morphology. The first component captured primarily global and cortical brain measures, coupled to glycoprotein acetyls and HDL. Glycoprotein acetyls, a marker of inflammation, was found to have the strongest individual associations throughout our analyses. Cardiometabolic and brain disorders are commonly characterized by low-grade inflammation,^{38–40} which has been shown to have detrimental effects on brain morphology, particularly in temporal and frontal regions,⁴¹ in accordance with our findings. The effect direction was thereby opposite to that of HDL markers, fitting with a large body of research that defects in brain HDL metabolism play a role in all major neurodegenerative disorders.⁴² Indeed, our findings on the bidirectional causal effects involving these markers dovetail with promising reports of HDL-based therapies for brain disorders.⁴² The second component was associated with larger ventricles and smaller subcortical volumes, which are typical regional patterns of neurodegeneration, coupled to low LDL. This direction of the loadings thereby matches a previous study on the relation between LDL and brain volume.¹⁸ Notably, this study found that these associations were driven by elderly individuals and hypothesized that the lower LDL levels reflected disruption of cholesterol production due to neurodegeneration.^{18,43} This also agrees with our MR findings, indicating that these subcortical volumes have a causal effect on metabolite concentrations.

Coupling the identified cortical patterns to previously published brain maps enabled us to identify brain systems that are likely to interplay with the metabolic markers, based on similarity of their spatial distribution. While the same general systems were identified across the cortical maps, the directionality of their correlations and the specific receptors identified were different. Most notable was the identification of monoaminergic transporters and receptors, which play differential roles in regulating satiety and energy expenditure.⁴⁴ These systems are known to interact with inflammatory processes⁴⁵ and

lipoprotein levels, as well as influence neuron proliferation, explaining the identified patterns. Such analyses thus provide further indications of the biological pathways involved in the relationship between metabolic processes and brain morphology that fit well with known functions of the identified molecular correlates. We note that the set of maps available for comparison is limited at this time; expansion may provide further opportunities to identify important pathways.

We found robust indications of causal effects of the metabolites on brain morphology and *vice versa*. The majority of effects were found for metabolites on brain morphology, particularly in temporal and frontal regions, in line with the notion that metabolic processes are essential regulators of the development and maintenance of cortical morphology. Notably, in the other direction, the analyses indicated that specific medial frontal and subcortical regions have a causal effect on metabolite concentrations. This fits well with the known functions of these regions, broadly making up the central autonomic network, in top-down control of energy expenditure through goal-directed behaviour and physiological processes.⁴⁶ The hypothalamus (encompassed by the ventral diencephalon) and the brainstem are the brain's control centers of metabolic activity, yet we found few causal effects here. These regions consist of subnuclei that interact with each other and other brain regions through intricate negative feedback loops that stimulate or inhibit feeding and regulate many physiological processes.¹³ As such, mixed effect directions across the nuclei are likely to obscure the full extent of effects in these regions; future studies may take advantage of more fine-grained parcellation^{47,48} to delve deeper into this.

Strengths of this study consist of a sample size an order of magnitude larger than any previous study of human neurometabolomics, and the use of comprehensive, accurately measured targeted metabolomics data. We further combined a range of statistical approaches to provide insight into shared and specific causal relationships between metabolites and well-established measures of brain morphology. The resulting summary statistics provide an atlas of associations, per metabolite and per brain region, that can drive targeted follow-up research. We were limited by measurement of metabolite concentrations in plasma, rather than in brain tissue, and the two have been shown to have a relatively low correlation.⁴⁹ However, the easy accessibility of plasma measures makes them much more feasible as biomarkers, and this data likely more directly reflects current metabolic state. We further did not look into age-related effects across the lifespan, which may obscure interesting effects, given the known dynamic nature of metabolic activity in the brain, e.g. from animal models.⁵⁰

In conclusion, we have shown that plasma markers of metabolic processes can be leveraged to better understand biological pathways underlying brain morphology. The identified causal relationships strongly indicate the crucial role of tagged metabolic processes in brain development and maintenance. We have generated an atlas of associations and causal relationships that enable a range of follow-up research into specific subsets of markers and biological pathways. We have provided insights into the role of metabolic processes in brain health, which is likely to be essential to better understand both neurodevelopment and neurodegeneration.

References

1. Camandola, S. & Mattson, M. P. Brain metabolism in health, aging, and neurodegeneration. *EMBO J.* **36**, 1474–1492 (2017).
2. Vancampfort, D. *et al.* Risk of metabolic syndrome and its components in people with schizophrenia and related psychotic disorders, bipolar disorder and major depressive disorder: a systematic review and meta-analysis. *World Psychiatry* **14**, 339–347 (2015).
3. Santiago, J. A. & Potashkin, J. A. The impact of disease comorbidities in Alzheimer’s disease. *Front. Aging Neurosci.* **13**, 631770 (2021).
4. Julkunen, H. *et al.* Atlas of plasma NMR biomarkers for health and disease in 118,461 individuals from the UK Biobank. *Nat. Commun.* **14**, 604 (2023).
5. Buerge, T. *et al.* Metabolomic profiles predict individual multidisease outcomes. *Nat. Med.* **28**, 2309–2320 (2022).
6. Saklayen, M. G. The global epidemic of the metabolic syndrome. *Curr. Hypertens. Rep.* **20**, 1–8 (2018).
7. Bélanger, M., Allaman, I. & Magistretti, P. J. Brain Energy Metabolism: Focus on Astrocyte-Neuron Metabolic Cooperation. *Cell Metab.* **14**, 724–738 (2011).
8. Teleanu, R. I. *et al.* Neurotransmitters—key factors in neurological and neurodegenerative disorders of the central nervous system. *Int. J. Mol. Sci.* **23**, 5954 (2022).
9. Bruce, K. D., Zsombok, A. & Eckel, R. H. Lipid processing in the brain: a key regulator of systemic metabolism. *Front. Endocrinol.* **8**, 60 (2017).
10. Yoon, J. H. *et al.* Brain lipidomics: From functional landscape to clinical significance. *Sci. Adv.* **8**, eadc9317 (2022).
11. Müller, C. P. *et al.* Brain membrane lipids in major depression and anxiety disorders. *Biochim. Biophys. Acta BBA-Mol. Cell Biol. Lipids* **1851**, 1052–1065 (2015).
12. Bazinet, R. P. & Layé, S. Polyunsaturated fatty acids and their metabolites in brain function and disease. *Nat. Rev. Neurosci.* **15**, 771–785 (2014).
13. Gao, Q. & Horvath, T. L. Neurobiology of feeding and energy expenditure. *Annu Rev Neurosci* **30**, 367–398 (2007).
14. Delezie, J. & Handschin, C. Endocrine crosstalk between skeletal muscle and the brain. *Front. Neurol.* **9**, 698 (2018).
15. Gurholt, T. P. *et al.* Population-based body–brain mapping links brain morphology with anthropometrics and body composition. *Transl. Psychiatry* **11**, 1–12 (2021).
16. Kennedy, K. G. *et al.* Elevated lipids are associated with reduced regional brain structure in youth with bipolar disorder. *Acta Psychiatr. Scand.* **143**, 513–525 (2021).
17. Ward, M. A. *et al.* Low HDL cholesterol is associated with lower gray matter volume in cognitively healthy adults. *Front. Aging Neurosci.* **2**, 29 (2010).
18. Moazzami, K. *et al.* Association of mid-life serum lipid levels with late-life brain volumes: The atherosclerosis risk in communities neurocognitive study (ARICNCS). *Neuroimage* **223**, 117324 (2020).
19. Gordon, S. *et al.* Metabolites and MRI-Derived Markers of AD/DRD Risk in a Puerto Rican Cohort. *Res. Sq.* (2024).
20. Kindler, J. *et al.* Dysregulation of kynurenine metabolism is related to proinflammatory cytokines, attention, and prefrontal cortex volume in schizophrenia. *Mol. Psychiatry* **25**, 2860–2872 (2020).
21. Henkel, N. D. *et al.* Schizophrenia: A disorder of broken brain bioenergetics. *Mol. Psychiatry* **27**, 2393–2404 (2022).
22. Prabakaran, S. *et al.* Mitochondrial dysfunction in schizophrenia: evidence for compromised brain metabolism and oxidative stress. *Mol. Psychiatry* **9**, 684–697 (2004).
23. Du, F. *et al.* In Vivo Evidence for Cerebral Bioenergetic Abnormalities in Schizophrenia Measured Using 31P Magnetization Transfer Spectroscopy. *JAMA Psychiatry* **71**, 19–27 (2014).
24. Zeng, Y., Guo, R., Cao, S. & Yang, H. Causal associations between blood lipids and brain structures: a Mendelian randomization study. *Cereb. Cortex* **33**, 10901–10908 (2023).
25. Lin, B. D. *et al.* Dissecting causal relationships between cortical morphology and neuropsychiatric disorders: a bidirectional Mendelian randomization study. *medRxiv* 2024–09 (2024).
26. Desikan, R. S. *et al.* An automated labeling system for subdividing the human cerebral cortex on MRI scans into gyral based regions of interest. *NeuroImage* **31**, 968–980 (2006).
27. Fischl, B. *et al.* Whole brain segmentation: automated labeling of neuroanatomical structures in the human brain. *Neuron* **33**, 341–355 (2002).
28. van der Meer, D. *et al.* Pleiotropic and sex-specific genetic architecture of circulating metabolic markers. *medRxiv* 2024.07.30.24311254 (2024).
29. Bethlehem, R. A. I. *et al.* Brain charts for the human

- lifespan. *Nature* (2022) doi:10.1038/s41586-022-04554-y.
30. Winkler, A. M. *et al.* Cortical thickness or grey matter volume? The importance of selecting the phenotype for imaging genetics studies. *NeuroImage* **53**, 1135–1146 (2010).
 31. Grasby, K. L. *et al.* The genetic architecture of the human cerebral cortex. *bioRxiv* 399402–399402 (2018) doi:10.1101/399402.
 32. Xing, L., Huttner, W. B. & Namba, T. Role of cell metabolism in the pathophysiology of brain size-associated neurodevelopmental disorders. *Neurobiol. Dis.* **199**, 106607 (2024).
 33. Xing, L. *et al.* Functional synergy of a human-specific and an ape-specific metabolic regulator in human neocortex development. *Nat. Commun.* **15**, 3468 (2024).
 34. Rakic, P. Evolution of the neocortex: a perspective from developmental biology. *Nat. Rev. Neurosci.* **10**, 724–735 (2009).
 35. Deery, H. A., Di Paolo, R., Moran, C., Egan, G. F. & Jamadar, S. D. Lower brain glucose metabolism in normal ageing is predominantly frontal and temporal: A systematic review and pooled effect size and activation likelihood estimates meta-analyses. *Hum. Brain Mapp.* **44**, 1251–1277 (2023).
 36. Zanto, T. P. & Gazzaley, A. Aging of the frontal lobe. *Handb. Clin. Neurol.* **163**, 369–389 (2019).
 37. Choi, M. *et al.* Comparison of neurodegenerative types using different brain MRI analysis metrics in older adults with normal cognition, mild cognitive impairment, and Alzheimer’s dementia. *PLoS One* **14**, e0220739 (2019).
 38. Silveira Rossi, J. L. *et al.* Metabolic syndrome and cardiovascular diseases: Going beyond traditional risk factors. *Diabetes Metab. Res. Rev.* **38**, e3502 (2022).
 39. Uptegrove, R. & Khandaker, G. M. Cytokines, oxidative stress and cellular markers of inflammation in schizophrenia. *Neuroinflammation Schizophr.* 49–66 (2020).
 40. Więckowska-Gacek, A., Mietelska-Porowska, A., Wydrych, M. & Wojda, U. Western diet as a trigger of Alzheimer’s disease: From metabolic syndrome and systemic inflammation to neuroinflammation and neurodegeneration. *Ageing Res. Rev.* **70**, 101397 (2021).
 41. Williams, J. A. *et al.* Inflammation and brain structure in schizophrenia and other neuropsychiatric disorders: a Mendelian randomization study. *JAMA Psychiatry* **79**, 498–507 (2022).
 42. Turri, M., Marchi, C., Adorni, M. P., Calabresi, L. & Zimetti, F. Emerging role of HDL in brain cholesterol metabolism and neurodegenerative disorders. *Biochim. Biophys. Acta BBA-Mol. Cell Biol. Lipids* **1867**, 159123 (2022).
 43. Solomon, A. *et al.* Plasma levels of 24S-hydroxycholesterol reflect brain volumes in patients without objective cognitive impairment but not in those with Alzheimer’s disease. *Neurosci. Lett.* **462**, 89–93 (2009).
 44. Voigt, J.-P. & Fink, H. Serotonin controlling feeding and satiety. *Behav. Brain Res.* **277**, 14–31 (2015).
 45. Shajib, M. & Khan, W. The role of serotonin and its receptors in activation of immune responses and inflammation. *Acta Physiol.* **213**, 561–574 (2015).
 46. Benarroch, E. E. The central autonomic network: functional organization, dysfunction, and perspective. in *Mayo clinic proceedings* vol. 68 988–1001 (Elsevier, 1993).
 47. Billot, B. *et al.* Automated segmentation of the hypothalamus and associated subunits in brain MRI. *Neuroimage* **223**, 117287 (2020).
 48. Iglesias, J. E. *et al.* Bayesian segmentation of brainstem structures in MRI. *Neuroimage* **113**, 184–195 (2015).
 49. Huo, Z. *et al.* Brain and blood metabolome for Alzheimer’s dementia: findings from a targeted metabolomics analysis. *Neurobiol. Aging* **86**, 123–133 (2020).
 50. Ding, J. *et al.* A metabolome atlas of the aging mouse brain. *Nat. Commun.* **12**, 6021 (2021).
 51. Sudlow, C. *et al.* UK biobank: an open access resource for identifying the causes of a wide range of complex diseases of middle and old age. *PLoS Med.* **12**, e1001779–e1001779 (2015).
 52. Manichaikul, A. *et al.* Robust relationship inference in genome-wide association studies. *Bioinformatics* **26**, 2867–2873 (2010).
 53. Ritchie, S. C. *et al.* Quality control and removal of technical variation of NMR metabolic biomarker data in ~120,000 UK Biobank participants. *Sci. Data* **10**, 64–64 (2023).
 54. Beasley, T. M., Erickson, S. & Allison, D. B. Rank-based inverse normal transformations are increasingly used, but are they merited? *Behav. Genet.* **39**, 580–595 (2009).
 55. Bowden, J., Davey Smith, G., Haycock, P. C. & Burgess, S. Consistent estimation in Mendelian randomization with some invalid instruments using a weighted median estimator. *Genet. Epidemiol.* **40**, 304–314 (2016).
 56. Burgess, S. & Thompson, S. G. Interpreting findings from Mendelian randomization using the MR-Egger method. *Eur. J. Epidemiol.* **32**, 377–389 (2017).
 57. Friedman, J., Hastie, T. & Tibshirani, R. Regularization paths for generalized linear models via coordinate descent. *J. Stat. Softw.* **33**, 1 (2010).
 58. Markello, R. D. *et al.* Neuromaps: structural and functional interpretation of brain maps. *Nat. Methods* **19**, 1472–1479 (2022).

Methods

Study sample

We obtained UKB data under accession number 27412. The composition, set-up, and data gathering protocols of the UKB have been extensively described elsewhere.⁵¹ It has received ethics approval from the National Health Service National Research Ethics Service (ref 11/NW/0382), and obtained informed consent from its participants. We selected unrelated participants (KING cut-off 0.0884)⁵² that had both the Nightingale NMR metabolomics data and that underwent the brain MRI protocol, as well as complete covariate data available (N=24,940, mean age at scan 64.0 years (SD=7.5), 52.5 % female).

Data preprocessing

We used Freesurfer to process the T1-weighted brain MRI data, using the default recon-all pipeline. For the main analyses, we focused on regions of interest for ease of interpretation: from the cortical stream, we extracted 34 regional cortical thickness and surface area measures based on the Desikan-Killiany cortical atlas, together with mean cortical thickness and total surface area. From the subcortical stream, we selected 21 regional measures of interest, together with ICV. For all hemisphere-specific measures, we summed the estimates from left and right together, in order to improve signal-to-noise and reduce the multiple-comparisons correction burden.

We further excluded all individuals with bad quality scans, as determined by an age- and sex-corrected Euler number more than three deviations below the scanner mean. Next, we pre-residualized each MRI measure for sex, age at baseline (the time when the blood sample for metabolomics data was taken), age at scan, scanner, and Euler number. For the regional measures, we also regressed out a metric-specific global measure: mean cortical thickness for regional thickness, total surface area for regional area, and ICV for the subcortical measures.

We conducted additional pre-processing through the ‘ukbnmr’ R package to the NMR data as released by UKB, to remove sources of technical noise.⁵³

We applied rank-based inverse normal transformation to both the residualized MRI data and metabolomics data,⁵⁴ leading to normally distributed measures.

Regression analyses

For the main analyses, we ran simple linear regression analyses, regressing each pre-residualized brain measure onto each marker, extracting the beta, standard error, p-value and r^2 from the model output. Correlations were calculated as the square root of the r^2 value, with the sign from the beta. Z-values were derived from the p-value and the sign of the beta. PLS regression was performed on each brain measure through the ‘regression’ mode of the ‘pls’ R package, including all markers as input terms. We extracted the maximum r^2 value from the model output.

Mendelian randomization

We conducted bidirectional two-sample MR by applying the *TwoSampleMR* R package to GWAS summary statistics. For the brain morphology measures, we ran GWAS on the full UKB sample of White European individuals with T1 MRI data (n=39,098) through PLINK2 with default settings, pre-residualizing for the same covariates as in the main analyses plus twenty genetic principal components. For the metabolic markers, we ran GWAS on each metabolic marker in UKB, excluding those individuals that were part of the neuroimaging GWAS sample (N=197,475, age 57.60 (SD 8.32), 53.84% female). We selected only genome wide significant variants for the analysis. We used the IVW MR results as main results, while leveraging weighted median⁵⁵ and MR-Egger⁵⁶ methods to check for robustness of findings.

LASSO

To examine the independent contribution of each marker on the brain measures we employed LASSO regression.⁵⁷ All 249 metabolic markers were included simultaneously into a regression model for each of the 91 pre-residualized brain measures. For this, we used the R package ‘glmnet’. The respective LASSO-specific tuning parameter λ controlled the overall strength of the penalty term. The optimal λ , corresponding to minimum deviance, was determined by performing 10-fold cross-validation.

Canonical correlation analysis

We applied CCA to investigate the multivariate associations between metabolic markers and regional brain measures. CCA involves finding canonical modes that maximize correlation between the linear combination of metabolic markers and the linear combination of brain measures. We extracted the first two dominant CCA modes of variation. These two orthogonal modes explained the largest fraction of correlation between metabolic and brain measurements.

Furthermore, we computed CCA loadings to quantify the contribution of each metabolic marker and each brain measure to the construction of the latent modes. These loadings are obtained as Pearson’s correlation between a respective subject-wise latent variable and the original measurement.

Neuromaps

We utilized the Neuromaps resource to contextualize brain maps derived from univariate and multivariate analyses.⁵⁸ Specifically, we compared them with previously published brain maps of molecular, structural, temporal and functional features. We first parcellated the curated set of reference maps using the Desikan-Killiany cortical atlas to ensure comparability. We then computed Pearson’s correlation between parcellated reference maps and our metabolic cortical spatial patterns as well as brain CCA modes.

Statistical analyses

All pre-processing steps and analyses performed outside the above-mentioned tools and software, e.g. formatting the data and creating the graphs, were carried out in R, v4.4. Where applicable, we adjusted p-values with the Benjamini-Hochberg method to correct for comparisons across the 249 markers and 91 brain measures, and set significance thresholds at $\alpha=.05$. All analyses were corrected for age, sex, scanner, and scan quality.

Acknowledgements

This work was partly performed on the TSD (Tjeneste for Sensitive Data) facilities, owned by the University of Oslo, operated and developed by the TSD service group at the University of Oslo, IT-Department (USIT). (tsd-drift@usit.uio.no). Computations were also performed on resources provided by UNINETT Sigma2 - the National Infrastructure for High-Performance Computing and Data Storage in Norway (NS9666S).

Materials & Correspondence

The data incorporated in this work were gathered from public resources. The code is available via <https://github.com/precimed> (GPLv3 license). Correspondence and requests for materials should be addressed to [d.v.d.meer\[at\]medisin.uio.no](mailto:d.v.d.meer[at]medisin.uio.no)

Conflicts of interest

OAA has received speaker's honorarium from Lundbeck, Janssen, Otsuka, and Sunovion and is a consultant to Cortechs.ai. and Precision Health. AMD was a Founder of and holds equity in CorTechs Labs, Inc, and serves on its Scientific Advisory Board. He is also a member of the Scientific Advisory Board of Human Longevity, Inc. (HLI), and the Mohn Medical Imaging and Visualization Centre in Bergen, Norway. He receives funding through a research agreement with General Electric Healthcare (GEHC). The terms of these arrangements have been reviewed and approved by the University of California, San Diego in accordance with its conflict-of-interest policies. All other authors report no potential conflicts of interest.

Financial support

The authors were funded by the Research Council of Norway (296030, 324252, 324499, 326813, 334920, 351751); the South-Eastern Norway Regional Health Authority (2020060); European Union's Horizon 2020 Research and Innovation Programme (Grant No. 847776; CoMorMent and Grant No. 964874; RealMent); EU's Horizon Psych-STRATA project (#101057454); National Institutes of Health (NIH; U24DA041123; R01AG076838; U24DA055330; and OT2HL161847).

Author contributions

D.v.d.M. and O.A.A. conceived the study; D.v.d.M. and J.K. pre-processed the data. D.v.d.M., J.K. and J.R. performed all analyses, with conceptual input from J.F.,

A.S., S.S., A.M.D., and O.A.A.; All authors contributed to interpretation of results; D.v.d.M. drafted the manuscript and all authors contributed to and approved the final manuscript.